



## LED biasing scheme with thermal compensation for automotive industry applications

J.R. Martínez-Pérez<sup>a</sup>, A. Martínez-Olmos<sup>b</sup>, J.J. Santaella<sup>a</sup>, P. Escobedo<sup>b</sup>, N. López-Ruiz<sup>b</sup>, M.A. Carvajal<sup>b,\*</sup>

<sup>a</sup> R&D Department, Valeo, 23600 Martos, Spain

<sup>b</sup> Department of Electronics and Computer Technology, ETSIT, University of Granada, 18014 Granada, Spain

### ARTICLE INFO

#### Keywords:

Automotive lighting  
Thermal compensation  
Integrated driver  
LED  
Thermistor

### ABSTRACT

This work introduces a novel scheme for driving light-emitting diodes (LEDs) with thermal compensation. The primary objective of the system is to address the issue of emitted light intensity drift caused by temperature variations, with a particular focus on the automotive industry. The developed technique proposes an alternative approach to the traditional thermal approach, which primarily focuses on heat dissipation. In contrast, the presented strategy utilizes a temperature-dependent element, such as a thermistor, to generate a reference current that increases with temperature. The generated current is then amplified by a commercial integrated driver and employed to bias the LEDs. Consequently, the reduction in the emitted light intensity resulting from an increase in the internal temperature of the LED is counterbalanced by an elevation in the bias current. The luminous flux model developed for the proposed system predicts the attainment of stable light intensity across a wide temperature range. The proposed strategy has been applied to three commercial LEDs commonly employed in automotive signal lighting to produce red, yellow, and white light. Experimental results confirm a significant reduction in the thermal dependence of the luminous flux, with reduction factor of temperature dependence ranging between 3.7 and 14.2 for the least and most temperature-sensitive LED models analyzed, respectively.

### 1. Introduction

Automotive lighting encompasses the various illumination functions present in motor vehicles, including both interior and exterior lighting. Exterior lighting covers front, rear, and signaling illumination. While automotive headlamps are intended to illuminate the forward scenario in reduced visibility conditions such as night-time, heavy rain, or fog, rear and signaling lights are used to provide optical communication with other participants in traffic, thereby enhancing safety [1].

The history of automotive lighting traces back to the utilization of kerosene as a light source [2]. With the advent of electrical lighting systems in the early 20th century, vehicle illumination of the vehicle transitioned to incandescent lamps based on tungsten filament bulbs, starting from 1908 [3]. Throughout the 20th century, the electric bulb underwent improvements and advancements. In the mid-1960s, halogen headlamp bulbs were introduced for the first time in automotive applications. By incorporating halogen gases into the bulb, the filament was able to burn brighter and hotter without compromising its lifespan

[4].

In 1991, high intensity discharge (HID) lighting was first introduced in production vehicles in Europe [5]. HID headlamps offer several advantages over tungsten filament-based bulbs, including longer lifespan, higher light intensity, improved beam patterns with higher intensity, increased color temperature of the light source, and enhanced durability of the light source [6]. Nevertheless, HID lamps require a very high voltage, necessitating the use of a ballast to achieve approximately 10 kV and regulate the lamp's electrical current [1]. This implies an increment in cost and safety risks due to the utilization of such high voltages, along with limited scalability possibilities. Currently, HID lamps are no longer employed in automotive lighting. Halogen headlamps remained the dominant choice until the emergence of solid-state (SS) lighting technology in the early 21st century, which displaced them [7]. Nowadays, the advancements in this technology have led to the widespread adoption of light emitting diodes (LEDs) for over 95 % of illumination functions in the automotive industry [8].

LEDs offer numerous advantages as light sources compared to

\* Corresponding author.

E-mail address: [carvajal@ugr.es](mailto:carvajal@ugr.es) (M.A. Carvajal).

previous illumination devices, with high efficiency being the most relevant. Efficiency is defined as the lumens emitted per watt, and white LEDs can reach values as high as 150 lm/W (with potential for further improvement). In contrast, HID lamps exhibit efficiency values up to 90 lm/W, while halogen bulbs are limited to values of 20–25 lm/W [1,9]. Additionally, LEDs present an extended lifespan. Other benefits of the solid-state illumination include high physical robustness and compactness, small size, light weight, a wide range of vivid colors, and absence of radiation in the ultraviolet and infrared spectra, among others [10].

However, SS lighting also presents certain drawbacks. LED-based lights can cause dazzle that affects pedestrians and other drivers due to the reduced size of the lamps [11,12]. Furthermore, SS lights exhibit a strong dependence with temperature, with only 20–40 % of the energy being converted into light [13], while most of the energy is transformed into heat. Heat dissipation arises not only from the LED itself, but also from the driving electronics and light conversion elements [14]. This heat dissipation produces a gradual temperature increase during the SS lamp operation, with the junction temperature of the LED, which refers to the temperature of the active region, being a critical parameter. The internal quantum efficiency of the LED depends on the junction temperature. Main mechanisms that lead to the decrease in the efficiency of the light output are related to non-radiative recombination through the well-known processes of Shockley-Read-Hall recombination and Auger recombination [15]. In addition, high-temperature operation shortens the device lifespan and can lead to the degradation of the encapsulant [15]. Ambient temperature also significantly affects the performance of the LEDs [10]. As a result, the luminous flux generated by a LED has a strong dependence on temperature.

Therefore, it is highly recommended to design SS lamps with efficient thermal management systems to mitigate these issues. Different strategies have been developed for this purpose. Some studies focus on predicting the junction temperature of the LED through thermal modelling [16–18]. Thermal characterization of the LED drivers and light conversion units has recently become the subject of investigation [19,20], and heat dissipation techniques have been implemented to maintain a constant temperature in SS lamps [21–23].

Special interest is devoted to maintaining a stable emitted light. Lamps used in automotive lighting must be designed to meet the color and luminosity limits established by the applicable regulations. In particular, the technical specifications for signal lights in automotive lighting, including rear-registration plate illuminating lamps, direction indicator lamps, position lamps, stop lamps, end-outline marker lamps, reversing lamps, manoeuvring lamps, rear fog lamps, parking lamps, daytime running lamps, and side marker lamps in the countries associated with the United Nations Economic Commission for Europe (UNECE), are detailed in the UN Regulations No. 148 and 149 [24]. It has also been determined that variations in the emitted light by the vehicles might lead to an increase of the accident rate and health risks [25,26].

Since the emitted light flux and the peak wavelength of an LED depend on the ambient temperature [15], some studies have focused on correcting not only the junction temperature of the SS lamp but also the drifts in the luminous flux caused by changes in ambient temperature [27,28]. Pena et al. [27] utilize two discrete currents, switching between them based on a specific temperature threshold, to increment the LED's bias current as the temperature rises. Karray et al. [28] increase the bias current in discrete steps when the light flux falls below a certain threshold. Both systems require a flux detector and logic to switch the bias current in discrete increments. Consequently, a microcontroller has been incorporated into the design to process the flux measurement and adjust the bias current accordingly.

In this work, we present an electronic system designed to address thermal compensation and correct light flux drifts in LEDs employed in automotive signal lighting with the aim of generating a stable light flux to meet the applicable regulations and to reduce risks in the automotive industry. The proposed system eliminates the need for threshold or flux

detectors and, instead, utilizes a thermistor and a resistor network to offer a straightforward yet effective analog solution based on passive devices. This approach avoids conflicts with more complex mechanisms involving microcontrollers and software, as seen in Refs. [27–30]. The primary objective of this research is to present an innovative, cost-effective, and reliable solution for low-power applications, using integrated current drivers and thermistors to compensate for the decrease in optical flux resulting from the operating temperature fluctuations in the LEDs. To validate our technique, we applied it to three common LEDs used in the development of signal lamps for automotive lighting (red, white, and yellow). The results demonstrate significant reduction in luminous flux drift caused by temperature variations in all three cases.

## 2. Technical background

In the design of SS lamps, particularly for the automotive industry, it is common to incorporate commercially available integrated current drivers, ensuring a constant current flow through the LED over a wide temperature and operating voltage ranges. These devices allow simple and easy operation of the LEDs in low-power applications with driving currents from 10 to 150 mA, thus avoiding complex designs with discrete components. Fig. 1 illustrates a standard circuit configuration for biasing LEDs in an SS lamp using an integrated current driver.

The integrated driver in Fig. 1 is a commercial device that regulates the power supply to one or more LEDs, providing a constant current whose intensity is configurable through an external resistor. Internally, this device implements one or several current sources for the biasing of the LEDs. The generated output current is determined by the external shunt resistor ( $R_S$ ) as stated in Equation (1).

$$I_{bias} = K \frac{V_{IR}}{R_S} \quad (1)$$

where  $V_{IR}$  represents the reference voltage of the driver and  $K$  denotes the constant current amplification factor specific to the integrated current driver employed, which is a fixed parameter for every commercial integrated driver. This design ensures a highly stable value for each current, enabling effective biasing of the LEDs. While it is commonly assumed that this configuration enables the lamp to provide a constant luminous flux, it is important to acknowledge that the junction temperature of the diodes significantly impacts this flux, as discussed in the Introduction section. It is a general well-known effect that high temperatures produce lower intensity of emitted light [31], with variations in this intensity exceeding 100 % possible across a broad temperature range.

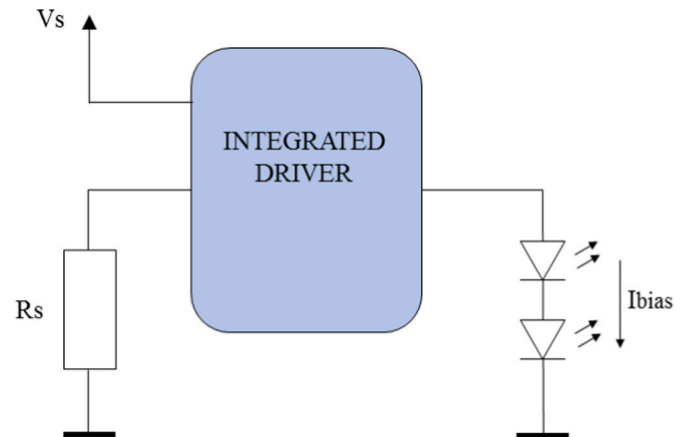


Fig. 1. Schematic representation of the fundamental topology for a linear current source used for driving LEDs, incorporating an integrated current driver.

The objective of this work is to modify the general design depicted in Fig. 1 in order to compensate for the effects produced by fluctuations in the internal temperature of the driven LEDs. The goal is to design a LED-driver system, using off-the-shelf integrated drivers, capable of generating a constant luminous flux, which differs from maintaining a constant current. Thermistors, which are temperature-dependent resistive passive components, have been widely employed for thermal compensation in various applications [32,33]. In this work, these devices are integrated into the driver system, enabling automatic adjustment of the bias current based on the temperature of the LEDs, thereby ensuring a stable light intensity.

### 3. Thermal model

To achieve a stable luminous flux, the driver system for LED biasing is designed to generate a current that varies in accordance with the temperature of the emitting diodes. The objective is to compensate for the drifts caused by such temperature fluctuations. As an initial approximation, the relationship between the biasing current and the intensity of the light emitted by an LED can be considered linear [34], according to Equation (2).

$$\varphi_r = a \cdot I \quad (2)$$

where  $\varphi_r$  represents the relative luminous flux,  $a$  denotes the proportionality constant, and  $I$  the current flowing through the LED. In addition,  $\varphi_r$  can be expressed as a function of temperature [35] when the bias current remains constant:

$$\varphi_r = e^{\alpha(T_j - T_{j0})} \quad (3)$$

where  $\alpha$  is the temperature coefficient of the LED,  $T_j$  represents its junction temperature, and  $T_{j0}$  denotes the reference junction temperature. By combining Equations (2) and (3), the drift in the luminous flux caused by changes in the internal temperature can be modelled as a thermal dependence of the biasing current in the form:

$$I_T = \frac{e^{\alpha(T_j - T_{j0})}}{a} = \frac{e^{-\alpha T_{j0}}}{a} \cdot e^{\alpha T_j} = \beta \cdot e^{\alpha T_j} \quad (4)$$

where  $\beta$  represents a constant value for a given current.

Hence, it becomes feasible to compensate for the thermal drift of the LED emitted light if the driving system can generate a bias current  $I_{bias}$  that follows the behaviour opposite to Equation (4), that is:

$$I_{bias} = I_0 \cdot e^{-\alpha T_j} \quad (5)$$

being  $I_0$  the constant factor encompassing the thermal dependence from Equation (4).

Since this current should be produced using a commercially available integrated driver, such as the one presented in Fig. 1, its value is determined based on Equation (1). Therefore, the external shunt resistor required to obtain the compensating current is given by:

$$R_S = K \frac{V_{IR}}{I_0} e^{\alpha T_j} \quad (6)$$

This indicates that a variable resistor, whose resistance value exponentially depends on the temperature, should be employed as the shunt resistor. Considering that  $\alpha$  is always negative for an LED, a negative temperature coefficient (NTC) thermistor is an appropriate device to accomplish this function. An NTC-thermistor is a well-known device commonly used to monitor the temperature in real-time applications [36], given that its nominal resistance value decreases exponentially with temperature:

$$R_{NTC} = R_0 \cdot e^{B \left( \frac{1}{T} - \frac{1}{T_0} \right)} \quad (7)$$

where  $R_{NTC}$  represents the resistance at the ambient absolute temperature  $T$ ,  $R_0$  signifies the resistance at temperature  $T_0$ , and  $B$  denotes the thermistor's constant.

As demonstrated in Equation (7), the thermal dependence of an NTC thermistor is expressed in terms of the inverse of temperature. To configure a resistance that varies with temperature in a similar manner as described in Equation (6), a resistive network incorporating the thermistor is proposed to be used as the required shunt resistor ( $R_S$ ) in the driver system of Fig. 1. This network is presented in Fig. 2.

The equivalent resistance of this network is calculated as:

$$R_{eq} = R_1 + R_{NTC} \parallel R_2 = R_1 + \frac{R_2 \cdot R_0 \cdot e^{B \left( \frac{1}{T} - \frac{1}{T_0} \right)}}{R_2 + R_0 \cdot e^{B \left( \frac{1}{T} - \frac{1}{T_0} \right)}} \quad (8)$$

The internal junction temperature of the LED ( $T_j$ ) is determined experimentally by means of a common indirect measurement method [37]. This method involves measuring the pad lead temperature ( $T_p$ ) and extrapolating it using the thermal resistance value ( $R_{th}$ ) provided by the LED manufacturer, along with the operating power ( $P$ ), to find the junction temperature through the following relationship:

$$T_j = T_p + R_{th} \cdot P \quad (9)$$

In the proposed driver system, the thermistor is placed close to the LED pad, so the ambient temperature  $T$  in Equation (7) corresponds to the pad temperature in Equation (9). As a result, Equation (8) can be expressed in terms of the junction temperature as:

$$R_{equ} = R_1 + \frac{R_2 \cdot R_0 \cdot e^{B \left( \frac{1}{T_j - R_{th} \cdot P} - \frac{1}{T_0} \right)}}{R_2 + R_0 \cdot e^{B \left( \frac{1}{T_j - R_{th} \cdot P} - \frac{1}{T_0} \right)}} \quad (10)$$

By appropriately selecting the parameters  $R_1$ ,  $R_2$ ,  $R_0$  and  $B$ , the behaviour of  $R_{eq}$  can closely resemble  $R_S$  from Equation (6) over a certain temperature interval. Consequently, it becomes possible to utilize a commercially available integrated driver for generating a current

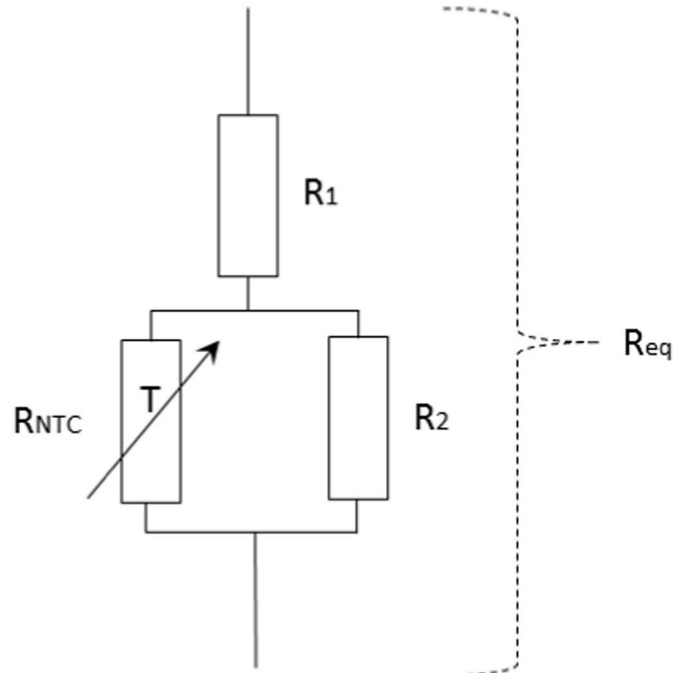


Fig. 2. Resistor network serving as the shunt resistance in the driving circuit.

that varies with temperature, thereby ensuring a stable luminous flux through the introduction of a resistive network comprising a thermistor as a resistive shunt in the driver configuration.

#### 4. Materials and methods

The model described in the previous section was applied to compensate for the thermal drift of the luminous flux resulting from temperature variations in three commonly used commercial LEDs for automotive lighting: DWA-MKG and DWY-MKG (Dominant Opto Technologies, Melaka, Malaysia), based on  $(Al_xGa_{1-x})_0.5In_{0.5}P$  technology; and NFSW172AT (Nichia Corporation, Tokushima, Japan), based on GaN technology. These LEDs emit red light ( $\lambda_p = 624$  nm), yellow light ( $\lambda_p = 587$  nm), and white light, respectively. This selection of LEDs covers the primary applications of exterior automotive lighting, such as headlamps and rearlamps. Three samples of each LED model were analyzed.

The integrated drivers employed for biasing the selected LEDs in this study are the E522.92 model for the red and yellow LEDs, and the E522.82 model for the white LED (Elmos Semiconductor, Dortmund, Germany). These drivers feature independent triple linear high-side current sources for LED driving and support allow parallel operation up to 165 mA and 450 mA, respectively.

To obtain the temperature coefficient for each LED model, the LEDs were subjected to optical characterization. This is a process in which the luminous flux of the LEDs is measured at various temperatures and different bias current to obtain comprehensive information about its thermal drift.

For this purpose, the LEDs and the drivers were mounted on a printed circuit board (PCB), as shown in Fig. 3(A). Three LEDs of each commercial model were used to obtain measurement replicas, and one PCB was fabricated for each model. These PCBs were placed within a climatic chamber model CTS T -70/600 (CTS GmbH, Kall, Germany), capable of generating stable temperature conditions ranging from  $-70$  °C to  $180$  °C (Fig. 3(B)).

The characterization began at the minimum temperature of  $-40$  °C and increased in steps of  $10$  °C until reaching the final temperature of  $70$  °C. At each temperature, a stabilization time of 120 min was imposed before measuring the luminous flux to ensure homogenous temperature distribution within the climatic chamber and the electronic components of the board.

Once the temperature stabilized in the chamber, the system, including three identical LEDs, was biased at different constant currents above and below the nominal forward current of the selected commercial models. For each current, the luminous flux of the three LEDs was acquired using an integrating sphere model SP23 (Feasa Enterprises, Limerick, Ireland). An LED spectrometer model S2 (Feasa Enterprises,

Limerick, Ireland) was connected to the integrating sphere, enabling light quantification and processing of the acquired data. This process was repeated for temperatures ranging from  $-40$  to  $70$  °C.

#### 5. Results

The results derived from the optical characterization of the LEDs are presented in Fig. 4, where the luminous flux of the three different analyzed LEDs is plotted across the temperature range of  $-40$  to  $70$  °C for various fixed biasing currents. As it can be seen, the expected reduction of the emitted luminous flux is appreciated as the temperature rises.

To extract the value of the thermal coefficient, Equation (3) was linearized under the assumption of low  $\alpha$  values and temperatures in proximity to  $T_{j0}$ :

$$\varphi_r - 1 = \alpha(T_j - T_{j0}) \tag{11}$$

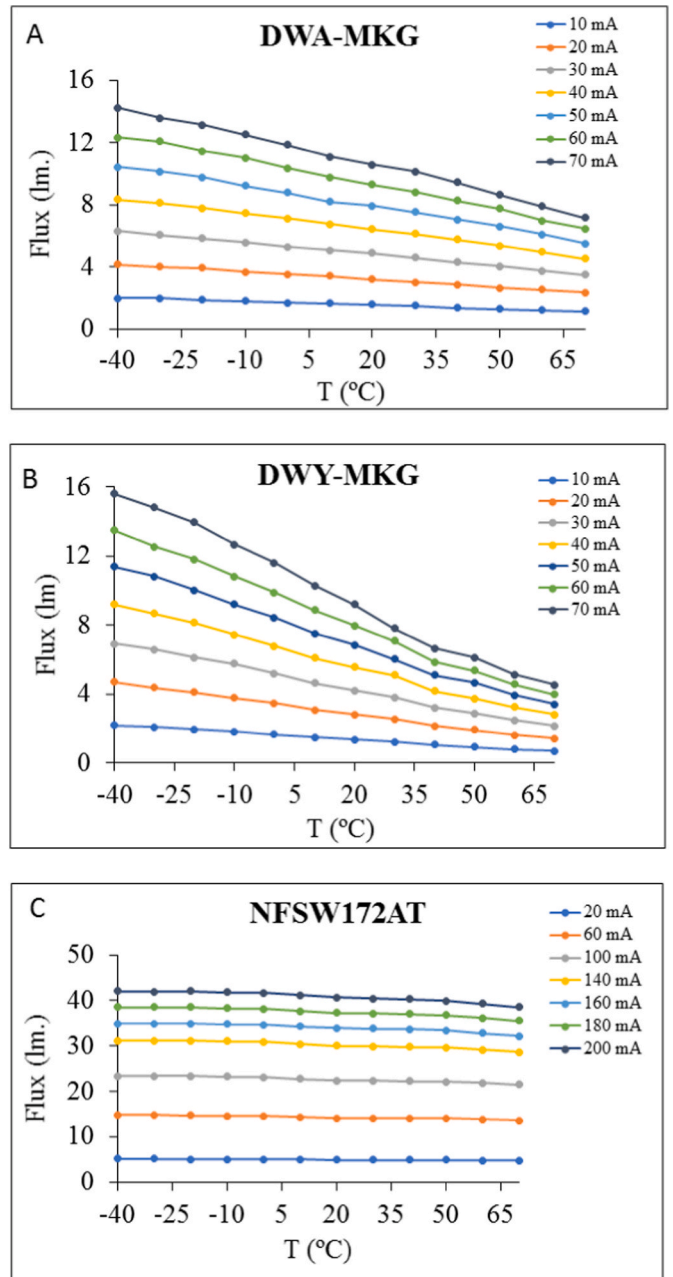


Fig. 4. Optical characterization of the LEDs.

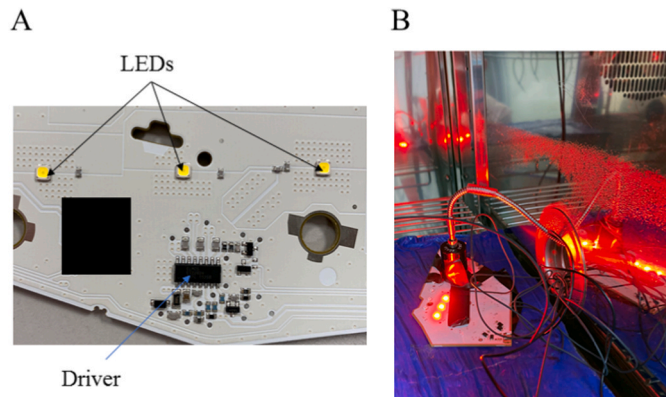


Fig. 3. PCB with the selected LEDs and integrated drivers (A). System placed inside the climatic chamber (B).



By applying Equation (11) to the data depicted in Fig. 4, the thermal coefficients of the LEDs were estimated. The obtained results are presented in Table 1.

With the resulting thermal coefficients, it is possible to determine required bias current values given by Equation (5) to compensate for the thermal drifts. These bias currents have been calculated for the three analyzed LEDs and are presented in Fig. 5 (blue line) for bias currents of 40 mA, 20 mA and 100 mA at 25 °C, respectively. As observed, the driving current needs to increase with the internal temperature to counteract the decrease in luminous flux caused by rising temperatures. To generate this current using the proposed system, consisting of a commercial integrated driver and the shunt resistor network (Fig. 2), the following resistance values were selected.

- Model DWA-MKG:  $R_0 = 10 \text{ k}\Omega$ ,  $R_1 = 4.7 \text{ k}\Omega$ ,  $R_2 = 35 \text{ k}\Omega$ .
- Model DWY-MKG:  $R_0 = 22 \text{ k}\Omega$ ,  $R_1 = 100 \text{ }\Omega$ ,  $R_2 = 100 \text{ k}\Omega$ .
- Model NFSW172AT:  $R_0 = 15 \text{ k}\Omega$ ,  $R_1 = 12 \text{ k}\Omega$ ,  $R_2 = 3.3 \text{ k}\Omega$ .

Here,  $R_0$  represents the resistance of the NTC at 25 °C. Using these values for the resistive network, the current that the system should generate can be calculated from Equations (6)–(8), resulting in the values shown in Fig. 5. In this Figure, the theoretical bias current generated by the biasing system depicted in Fig. 1, when the shunt resistance  $R_s$  follows an ideal exponential behaviour as described in Equation (6), is represented by the blue line. This bias current is required to compensate for the thermal dependence of the luminous flux, modelled in Equation (3). The dotted line in Fig. 5 shows the theoretical bias current that the integrated current driver generates if the shunt resistance is replaced by the resistances group of Fig. 2, which includes the thermal-sensitive element, the thermistor.

Fig. 5 shows that the required (blue line) and obtained (dotted line) results from the system are highly similar. Hence, it can be concluded that the proposed driving system should be capable of generating a driving current that compensates for the thermal drift of the luminous flux in the three LEDs.

For the physical implementation of the described resistive network, the NTC thermistors used were the NCP03XH103, NCP03XH223, and NCP03XH153 models (Murata Manufacturing, Nagaokakyō, Japan), which offer resistances at 25 °C of 10 kΩ, 22 kΩ and 15 kΩ, respectively.

A comprehensive parameter description of the selected components for the model described in the previous section is listed in Table 1.

The proposed driving circuit described in the previous section was successfully implemented using the components specified in Table 1. The LEDs biased with this circuit were subjected to optical characterization following the previously outlined methodology, which involved measuring the luminous flux within a temperature range of –40 to 60 °C. The obtained results are presented in Fig. 6. In this graph, the black

**Table 1**  
Component parameters.

LEDs		
DWA-MKG	DWY-MKG	NFSW172AT
$a$ (@40 mA) = 25 A <sup>-1</sup>	$a$ (@20 mA) = 50 A <sup>-1</sup>	$a$ (@100 mA) = 10 A <sup>-1</sup>
$\alpha = -0.0050 \pm 0.0006 \text{ K}^{-1}$	$\alpha = -0.011 \pm 0.002 \text{ K}^{-1}$	$\alpha = -0.0003 \pm 0.0001 \text{ K}^{-1}$
$R_{th} = 65 \text{ K/W}$	$R_{th} = 65 \text{ K/W}$	$R_{th} = 13.5 \text{ K/W}$
Integrated drivers		
ELMOS 522.82	ELMOS 522.92	
$K = 960$	$K = 311$	
$V_{IR} = 1.5 \text{ V}$	$V_{IR} = 1.5 \text{ V}$	
Thermistors		
NCP03XH103	NCP03XH223	NCP03XH153
$R_0 = 10 \text{ k}\Omega$	$R_0 = 22 \text{ k}\Omega$	$R_0 = 15 \text{ k}\Omega$
$T_0 = 25 \text{ }^\circ\text{C}$	$T_0 = 25 \text{ }^\circ\text{C}$	$T_0 = 25 \text{ }^\circ\text{C}$
$B = 3428 \text{ K}$	$B = 3428 \text{ K}$	$B = 3428 \text{ K}$

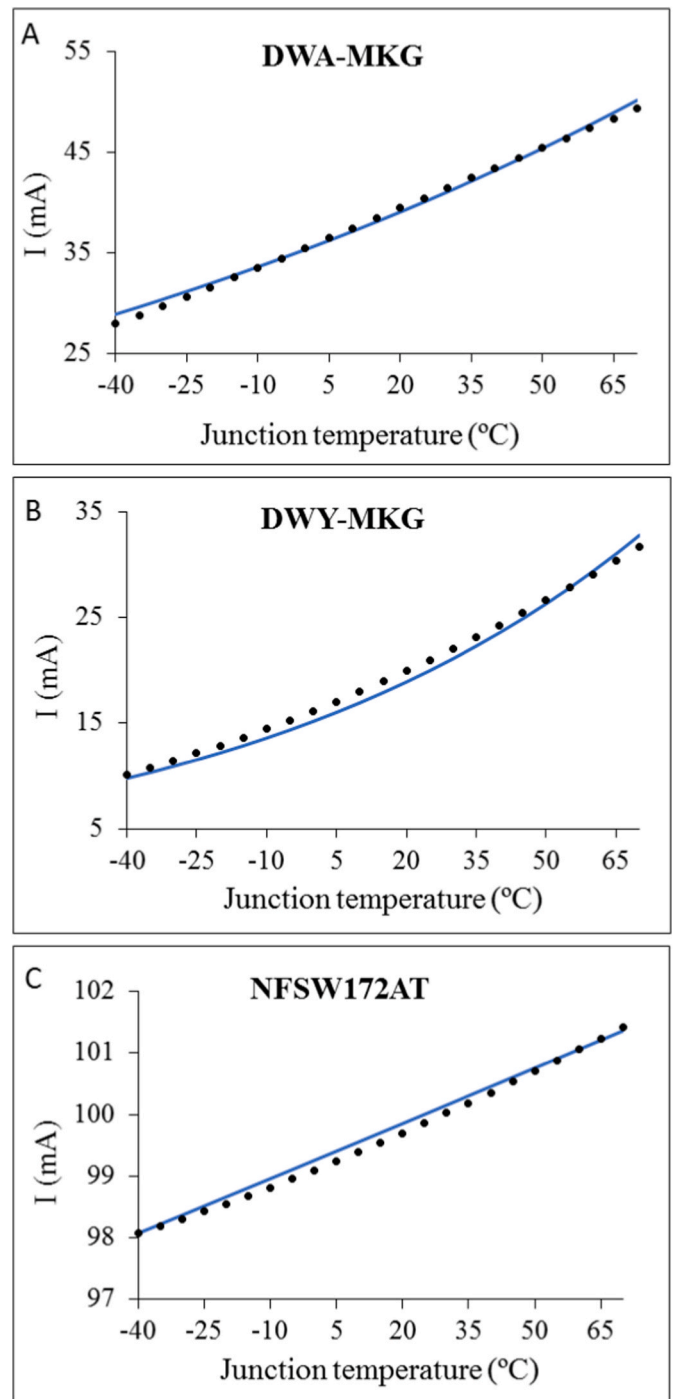


**Fig. 5.** Theoretical bias currents for thermal compensation: required (blue line) and calculated with the proposed model (black dots). (For interpretation of the references to color in this figure legend, the reader is referred to the Web version of this article.)

line represents the measured relative luminous flux obtained from the LEDs when the bias current is modified according to the junction temperature, indicating the thermally compensated luminous flux. The generated bias current required for this compensation is also depicted in Fig. 6 as the blue line. For comparison purposes, the relative luminous flux measured when the bias current is fixed at the nominal value specified by the manufacturer for each LED (40 mA, 20 mA, and 100 mA, respectively) is also included in the graph as the orange line.

As depicted, the relative flux within the evaluated temperature range remains more stable when the LEDs are biased through the proposed

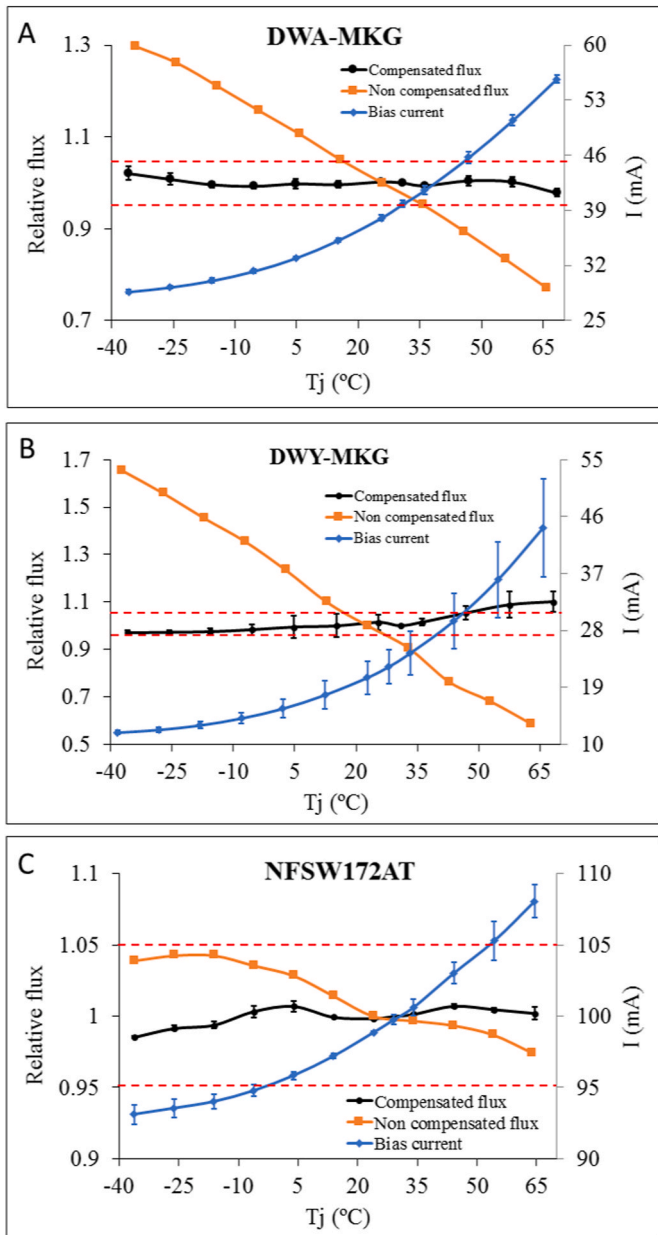


Fig. 6. Measured relative optical flux and bias current for thermal compensation.

system (black line) compared to the case of a constant bias current (orange line). As expected, this current increases with temperature to produce a corresponding increment in the emitted light, thereby compensating for the losses in luminous flux. In the event of higher temperatures, the current may reach the maximum current limit provided by the integrated driver. However, even under such circumstances, the LEDs would not be damaged as the maximum current is limited by the integrated driver. The applicable normative [24] stipulates that the actual luminous fluxes of each light source used should not deviate more than  $\pm 5\%$  from the mean value at the reference

temperature of 25 °C. These limits have been indicated in the graphics of Fig. 6 to demonstrate how the proposed compensation technique maintains the luminous flux within this interval across almost the entire temperature range.

As a figure of merit, Table 2 shows the maximum percentual variation of the relative flux  $\Delta\phi_r$  and its sensitivity to temperature  $\delta_r$  (obtained as the slope of the linear regression of the relative flux curves in Fig. 6) observed in the analyzed LEDs within the evaluated temperature range, considering the mean values across different replicas, for both compensated and non-compensated cases.

In light of these results, the significant enhancement in the stabilization of the luminous flux for the three selected LEDs becomes evident. The maximum flux deviation is reduced in a factor ranging from 14.2 to 3.7 while the sensitivity to temperature is reduced in more than 7 times in the worst case. It is noteworthy that the improvement is more evident for the LEDs exhibiting higher temperature dependence, whereas for the model less influenced by temperature (NFSW172AT), the level of stabilization is less pronounced. Furthermore, the different samples analyzed exhibit good repeatability in the results, with variations below 5 %.

For comparison purposes, the maximum variation of the luminous flux ( $\Delta\phi_r$ ) for the LED model DWA-MKG has been estimated when using a complex current driver that includes DC/DC converter and micro-controller for the control of the bias current in different temperature ranges. When thermal compensation is carried out through a device with these characteristics, the parameter  $\Delta\phi_r$  reaches a value above 50 %, which is significantly higher than the result obtained for the same LED with the thermal compensation technique presented here (4.2 %).

The luminous efficiency of the LED is defined as the rate between the luminous flux generated and the power supplied to the LED [15], as expressed in Equation (12).

$$\text{Luminous efficiency} = \frac{\Phi_{lum}}{I \cdot V} \quad (12)$$

This parameter strongly depends on the junction temperature, as the luminous flux decays with temperature, as explained in Section 3. When the bias current of the LED is fixed, the luminous efficiency depends solely on the external temperature, which ultimately affects the junction temperature, as expressed in Equation (9). Therefore, in this case, the luminous efficiency of the LED decreases with temperature. When the thermal compensation presented in this work is applied to the LED, the luminous flux generated remains more stable when the temperature varies. However, to achieve this stabilization, the bias current must increase when the temperature rises, as deduced from the results in Fig. 6. This increase in the bias current, following an exponential behaviour with temperature, leads to a higher power supplied to the device and, consequently, to a significant decrease in efficiency.

In both situations (biasing of the LED with thermal compensation or without compensation), the luminous efficiency decreases with temperature. In the case of thermal compensation, this decrease is expected to be more pronounced at high temperatures. The luminous efficiency of the LEDs analyzed in this work has been evaluated in the temperature range of  $-40$  to  $60$  °C, and the results are presented in Fig. 7. As it can be seen, the efficiency decreases with temperature in both compensated and non-compensated biasing, as expected. However, in the compensated case, higher values are achieved for most of the studied range, especially for at temperatures.

The proposed technique adjusts the bias current based on the actual

Table 2  
Maximum variations ( $\Delta\phi_r$ ) and sensitivity to temperature ( $\delta_r$ ) of the relative luminous flux.

LED model	$\Delta\phi_r$ (non-compensated)	$\Delta\phi_r$ (compensated)	$\delta_r$ (non-compensated)	$\delta_r$ (compensated)
DWA-MKG	59.7 %	4.2 %	$5.3 \cdot 10^{-3} \text{ } ^\circ\text{C}^{-1}$	$0.2 \cdot 10^{-3} \text{ } ^\circ\text{C}^{-1}$
DWY-MKG	115.0 %	13.1 %	$11 \cdot 10^{-3} \text{ } ^\circ\text{C}^{-1}$	$1.2 \cdot 10^{-3} \text{ } ^\circ\text{C}^{-1}$
NFSW172AT	8.2 %	2.2 %	$0.7 \cdot 10^{-3} \text{ } ^\circ\text{C}^{-1}$	$0.1 \cdot 10^{-3} \text{ } ^\circ\text{C}^{-1}$

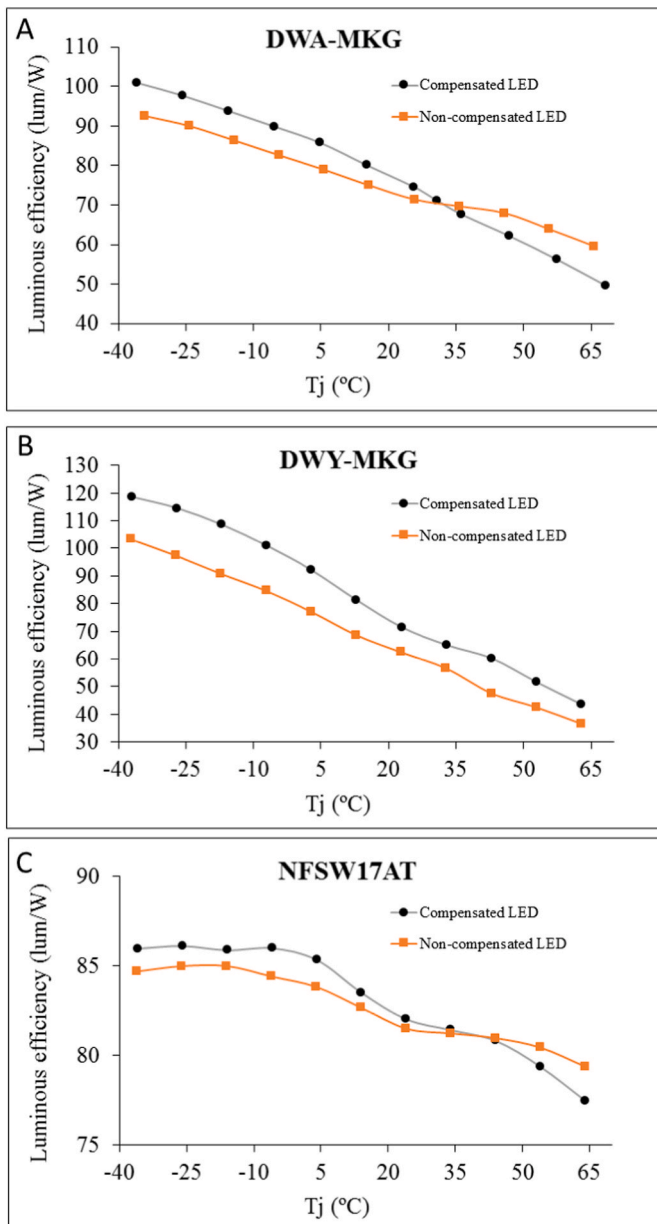


Fig. 7. Luminous efficiency of the LEDs.

junction temperature of the LEDs to maintain a stable luminous flux, as can be observed in the results shown in Fig. 6. At lower temperatures, the bias current is reduced below the nominal value provided by the manufacturer, which reduces the electrical stress on the LEDs. Conversely, at higher temperatures, the current is exponentially increased. While this elevated current may induce electrical stress that could potentially reduce the LEDs' service life, it is essential to note that the bias current is limited by the driver to values within the specifications of the LEDs. Therefore, the service life of the LEDs (L90B10, longer than 100.000 h) is guaranteed even in environments with temperatures up to 70 °C.

## 6. Conclusions

This paper presents a novel scheme for thermal compensation of the luminous flux generated by commonly used commercial LEDs in the automotive industry. The proposed approach offers a purely hardware-based analog solution, eliminating the need for microcontroller-based systems or software applications for adjusting the output flux through

current amplitude modulation (as opposed to other methods such as PWM adjustment) and without requiring light flux detectors. The developed solution utilizes an integrated current driver that incorporates a temperature-dependent element, specifically an NTC thermistor, to generate a reference current that is amplified to bias the LEDs. This element produces a variation of the current with temperature, thereby counterbalancing the decrease in the emitted light of the LED as the temperature rises. The proposed compensation technique has been applied to three commonly used LED models in automotive lighting (DWA-MKG, DWY-MKG, and NFSW172AT). The results show that the generated luminous flux in all cases remains much more stable in a wide temperature range from -40 to 60 °C compared to when the LEDs are biased with a fixed current. The maximum variations in luminous flux are reduced by 14.2, 8.8, and 3.7 times, respectively. The relative flux variation is limited to 13.1 % in the worst case. Additionally, the sensitivity of the relative luminous flux to temperature is reduced by 26.5, 9.2, and 7 times for the three LEDs. The thermal drift compensation technique also provides better luminous efficiency for the LEDs in all three cases at temperatures below 25–35 °C. With the proposed technique to compensate for thermal drifts in the luminous flux, the three models of LED analyzed in this work meet these legal requirements not only at the reference temperature but throughout almost the entire range of -40 to 60 °C.

## CRedit authorship contribution statement

**J.R. Martínez-Pérez:** Writing - original draft, Methodology, Investigation, Conceptualization. **A. Martínez-Olmos:** Writing - review & editing, Writing - original draft, Supervision, Investigation. **J.J. Santalla:** Methodology, Investigation, Conceptualization. **P. Escobedo:** Writing - review & editing, Writing - original draft, Investigation. **N. López-Ruiz:** Methodology, Investigation. **M.A. Carvajal:** Supervision, Project administration, Investigation, Conceptualization.

## Declaration of competing interest

The authors declare that they have no known competing financial interests or personal relationships that could have appeared to influence the work reported in this paper.

## Data availability

Data will be made available on request.

## Acknowledgments

This work has been developed with the support of the Valeo-UGR Chair and H2020 ELICSIR project (grant No. 857558). P. Escobedo thanks project IJC2020-043307-I funded by MCIN/AEI/10.13039/501100011033 and by "European Union NextGenerationEU/PRTR". The authors thank the technical assistance and the availability of VALEO ESPAÑA facilities in Martos, Spain, where the measurements were carried out.

## References

- [1] T.Q. Khanh, J. Kobbert, *Automotive front lighting system (status 2020)*, in: *Encyclopedia of Color Science and Technology*, Springer, Berlin, 2020.
- [2] J. Drach, *Automobilia, Automobil-teile und Zubehor von 1886 bis 1976, Band II*, Robert Bosch GmbH, Stuttgart, Germany, 1993.
- [3] E. R. Carlson, *the incandescent lamp for automotive lighting (SAE technical paper series No. 290048)*, warrendale, PA: society of automotive engineers, 1929, in: G. J. Gaudaen (Ed.), *Motor Vehicle Lighting*, Society of Automotive Engineers, Warrendale, PA, 1996, pp. 415–419.
- [4] B. Wördenweber, P. Boyce, D.D. Hoffman, J. Wallaschek, *Automotive lighting - state of the art*, in: *Automotive Lighting and Human Vision*, Springer-Verlag, Berlin, 2007.
- [5] W. Huhn, G. Hege, *High Intensity Discharge Headlamps (HID)—experience for More than 3-1/2 Years of Commercial Application of Litronic Headlamps (SAE*

- Technical Paper Series No. 950591), Society of Automotive Engineers, Warrendale, PA, 1995.
- [6] D.W. Moore, Headlamp History and Harmonization, Report No. UMTRI-98-21, the University of Michigan, Transportation Research Institute, Ann Arbor, 1998. June.
  - [7] C.C. Wen, C. Hsien Chen, H.Y. Lee, S.H. Chang, Y.C. Fang, A study of optical design of automotive lighting system with laser source, *J. Internet Technol.* 21 (7) (2020) 2039–2044, <https://doi.org/10.3966/160792642020122107018>.
  - [8] M. Kilic, M. Aktas, G. Sevilgen, Liquid cooling performance of the single and multi-led circuit boards used in automotive lighting systems, in: 4th International Conference on Smart and Sustainable Technologies, SpliTech, 2019, pp. 1–5, <https://doi.org/10.23919/SpliTech.2019.8783136>.
  - [9] A.N. Altarawneh, T.K. Murtadha, Managing engineering challenges in the design and implementation of eco-friendly residential structures, *Results Eng* 19 (2023), 101363, <https://doi.org/10.1016/j.rineng.2023.101363>.
  - [10] A. Almeida, B. Santos, B. Paolo, M. Quicheron, Solid state lighting review – potential and challenges in Europe, *Renewable Sustainable Energy Rev.* 34 (2014) 30–48, <https://doi.org/10.1016/j.rser.2014.02.029>.
  - [11] L. Erdem, K. Trampert, C. Neumann, Evaluation of discomfort glare from LED lighting systems, *Ingenieria Iluminatului* 14 (2) (2012) 17–26.
  - [12] T. Tashiro, S. Kawanobe, T. Kimura-Minoda, S. Kohko, T. Ishikawa, M. Ayama, Discomfort glare for white LED light sources with different spatial arrangements, *Light. Res. Technol.* 47 (3) (2015) 316–337, <https://doi.org/10.1177/1477153514532122>.
  - [13] J.Y. Tsao, M.E. Coltrin, M.A. Crawford, J.A. Simmons, Solid-state lighting: an integrated human factors, technology, and economic perspective, *Proc. IEEE* 98 (7) (2010) 1162–1179, <https://doi.org/10.1109/JPROC.2009.2031669>.
  - [14] W.D. van Driel, X.J. Fan, *Solid State Lighting Reliability in Components and Systems*, Springer, New York, 2013.
  - [15] E. Fred Schubert, *Junction and carrier temperatures*, in: *Light-Emitting Diodes*, second ed., Cambridge University Press, Cambridge, 2006.
  - [16] J. Li, Q. Yang, P. Niu, L. Jin, B. Meng, Y. Li, Z. Xiao, X. Zhang, Analysis of thermal field on integrated LED light source based on COM-SOL multi-physics finite element simulation, *Phys. Procedia* 22 (2011) 150–156, <https://doi.org/10.1016/j.phpro.2011.11.024>.
  - [17] J. Formanek, J. Jakovenko, Thermal characterization and lifetime prediction of LED boards for SSL lamp, *Radioengineering* 22 (1) (2013) 245–250.
  - [18] M. Cai, et al., Junction temperature prediction for led luminaires based on a subsystem-separated thermal modeling method, *IEEE Access* 7 (2019) 119755–119764, <https://doi.org/10.1109/ACCESS.2019.2936924>.
  - [19] J. Zhou, X.M. Long, J.G. He, L. Fang, X. Li, System-level thermal design for LED automotive lamp-based multiobjective simulation, *IEEE Trans. Compon. Packag. Manuf. Technol.* 7 (4) (2017) 591–601, <https://doi.org/10.1109/TCPMT.2017.2657580>.
  - [20] X. Perpiñá, et al., Thermal analysis of LED lamps for optimal driver integration, *IEEE Trans. Power Electron.* 30 (7) (2015) 3876–3891, <https://doi.org/10.1109/TPEL.2014.2346543>.
  - [21] X. Perpiñá, et al., Thermal management strategies for low- and high-voltage retrofit led lamp drivers, *IEEE Trans. Power Electron.* 34 (4) (2019) 3677–3688, <https://doi.org/10.1109/TPEL.2018.2853119>.
  - [22] M. Maaspuro, Novel ideas for thermal management of filament LED light bulbs, *Int. J. Online Biomed. Eng.* 17 (8) (2021) 60–73, <https://doi.org/10.3991/ijoe.v17i08.23695>.
  - [23] E.D. Jung, Y.L. Lee, Development of a heat dissipating LED headlamp with silicone lens to replace halogen bulbs in used car, *Appl. Therm. Eng.* 86 (2015) 143–150, <https://doi.org/10.1016/j.applthermaleng.2015.04.044>.
  - [24] UN Regulation No. 148 and 149, United Nations, Agreement Concerning the Adoption of Harmonized Technical United Nations Regulations for Wheeled Vehicles, Equipment and Parts Which Can Be Fitted And/or Be Used on Wheeled Vehicles and the Conditions for Reciprocal Recognition of Approvals Granted on the Basis of These United Nations Regulations, 2020. Revision 3, 9 January.
  - [25] B. Lehman, A.J. Wilkins, Designing to mitigate effects of flicker in led lighting: reducing risks to health and safety, *IEEE Power Energy Mag.* 1 (2014) 18–26, <https://doi.org/10.1109/MPEL.2014.2330442>.
  - [26] R. Palaniappan, S. Mouli, E. Fring, H. Bowman, I. McLoughlin, Incandescent bulb and LED brake lights: novel analysis of reaction times, *IEEE Access* 9 (2021) 29143–29152, <https://doi.org/10.1109/ACCESS.2021.3058579>.
  - [27] Pena, et al., Automotive Lamp with Compensation of the Luminous Flux of the Light Source, United States Patent no. US01048507SB2, 2019.
  - [28] M. Karrray, R. Taleb, H. El Idrissi, Method for Operating an Automotive Lighting Device and Automotive Lighting Device, Institut National de la Propriété Industrielle, no. de publication 3096579, 2019.
  - [29] C.P.G. Wong, A.T.L. Lee, K. Li, S.-C. Tan, S.Y. Hui, Precise luminous flux and color control of dimmable red-green-blue light-emitting diode systems, *IEEE Trans. Power Electron.* 37 (2022) 588–606, <https://doi.org/10.1109/TPEL.2021.3102260>.
  - [30] A.T.L. Lee, H. Chen, S.-C. Tan, S.Y.R. Hui, Non-linear Feedback Control of Robust Bi-color LED Lighting, *IEEE Energy Conversion Congress and Exposition (ECCE)*, Montreal, 2015, pp. 3215–3222, <https://doi.org/10.1109/ECCE.2015.7310112>. QC, Canada (2015).
  - [31] A. Poppe, C.J.M. Lasance, Standardization of LED thermal characterization, in: *Thermal Management for LED Applications*, Springer, Berlin, 2014.
  - [32] P. Atanasijevic, P. Mihailovic, Temperature compensation of NTC thermistors based anemometer, *Sens. Actuators, A* 285 (2019) 210–215, <https://doi.org/10.1016/j.sna.2018.11.004>.
  - [33] E. Kuznetsov, Temperature-compensated silicon photomultiplier, *Nucl. Instrum. Methods Phys. Res.: Accel. Spectrom. Detect. Assoc. Equip.* 912 (2018) 226–230, <https://doi.org/10.1016/j.nima.2017.11.060>.
  - [34] D. Peng, K. Liu, Modeling study of red LED spectral characteristics, *J. Phys.: Conf. Ser.* 1746 (2021), 012003, <https://doi.org/10.1088/1742-6596/1746/1/012003>.
  - [35] J. Yan, H. Liu, W. Zhao, Y. Su, Temperature Compensation for LED Filament Standard Lamps in Proc. SPIE 11189, Optical Metrology and Inspection for Industrial Applications VI, 111891N, 2019, <https://doi.org/10.1117/12.2537712>, 18 November.
  - [36] Md S. Shuvo, F. Ishtiaq, T. Jamee, J. Das, S. Saha, Analysis of internal cooling system in a vented cavity using P, PI, PID controllers, *Results Eng* 15 (2022), 100579, <https://doi.org/10.1016/j.rineng.2022.100579>.
  - [37] J. Bielecki, A.S. Jwania, F. El Khatib, T. Poorman, Thermal considerations for led components in an automotive lamp, in: *Twenty-Third Annual IEEE Semiconductor Thermal Measurement and Management Symposium*, 2007, pp. 37–43, <https://doi.org/10.1109/STHERM.2007.352403>.